Talanta 253 (2023) 124094

Contents lists available at ScienceDirect

Talanta

journal homepage: www.elsevier.com/locate/talanta

Thread-based microfluidic sensor for lithium monitoring in saliva

Izabela Lewińska [a], Luis Fermín Capitán-Vallvey [b,c], Miguel M. Erenas [b,c,*]

[a] University of Warsaw, Faculty of Chemistry, Pasteura 1, 02-093, Warsaw, Poland
[b] ECsens, Department of Analytical Chemistry, Campus Fuentenueva, Faculty of Sciences, 18071 University of Granada, Granada, Spain
[c] Unit of Excellence in Chemistry Applied to Biomedicine and the Environment of the University of Granada, 18071 University of Granada, Granada, Spain

ARTICLE INFO

Keywords:
Lithium
Thread-based analytical device
Ionophore-based optical sensors
Digital color analysis
Saliva analysis

ABSTRACT

Lithium administration is a commonly prescribed treatment for some mental disorders, e.g. bipolar disorder. However, Li^+ level must be regularly monitored to maintain therapeutical effect and avoid adverse side effects. Currently, it is determined in blood, using complex instrumentation, which excludes self-monitoring of lithium concentration by patients themselves. That creates a need for simple, reliable and fast sensors for Li monitoring in biological fluids. In this paper, we introduced a microfluidic thread-based analytical device for optical determination of lithium in saliva. Lithium ion recognition was achieved by incorporating of chromoionophore-ionophore chemistry onto thread. To ensure appropriate selectivity over other alkaline metal ions, it was necessary to include an efficient lithium extractant in the sensing cocktail, alongside its usual components. After optimization of cocktail composition, the developed sensors allowed for lithium determination in a range from $8.8{\cdot}10^{-4}$ to 0.95 mol L^{-1} with remarkable precision of 0.3% (at 10^{-2} mol L^{-1}) and within a very short time of ca. 10 s. The analytical usefulness of the developed sensors was tested with saliva samples, which were analyzed without any prior processing. A comparison of the obtained results with a reference method revealed high accuracy (relative error $< \pm 20\%$ in most cases).

1. Introduction

Lithium is a trace element with outstanding physiological properties. Its biochemistry draw attention because lithium possess mood-stabilizing, anti-viral, anti-inflammatory and neuroprotective features [1]. One of the most prevalent examples of its medical importance is lithium role in mental disorders treatment, especially bipolar disorder. Bipolar disorder is a disease affecting between 1 and 2% of world population although there are strong evidence that this percentage is underestimated [2]. This disease is characterized by recurrent episodes of depression and mania. In severe forms, it strongly affects patient's personal and social life. The gold standard treatment for both chronic and acute bipolar disorder is lithium supplementation, usually administrated in a form of lithium carbonate.

The major drawback of lithium as a therapeutic agent is that it is effective in a very narrow concentration range – from 0.4 to 1.2 mmol L^{-1} in serum. Concentration above 1.2 mmol L^{-1} cause severe side effects and can result in death. The most commonly reported side effects are: diarrhea and nausea, polyuria and polydipsia, tremor and weight gain. Sometimes lithium can also impair functioning of internal organs, such as kidneys or thyroid [3]. To ensure that the level of lithium remains within the therapeutic range, its concentration has to be frequently monitored for all patients undergoing treatment with lithium – 5 days after every dose adjustment and then every 3–6 months [4].

In a conventional approach lithium concentration is determined in blood serum, usually employing one of the following analytical methods – atomic absorption spectrometry, atomic emission spectrometry or potentiometry with Li ion-selective electrodes [5]. Such a procedure not only causes discomfort for the patient, but also relatively expensive and time-consuming. To avoid unpleasant blood collection, lithium can be alternatively determined in other matrices, like saliva, sweat, urine or interstitial fluid. Saliva seems to be one of the easiest to collect among mentioned above. Moreover, a few studies have established a correlation ($r =$ approx. 0.7) between lithium level in blood and in saliva [6,7], with the concentration of lithium in saliva being ca. Double its concentration in blood.

Because of high interest in more convenient lithium level control, much effort has been recently dedicated to the development of point-of-care sensors for lithium determination. Some examples are listed below. Komatsu et al. have reported a paper-based sensor for colorimetric

* Corresponding author. ECsens, Department of Analytical Chemistry, Campus Fuentenueva, Faculty of Sciences, 18071 University of Granada, Granada, Spain
E-mail address: erenas@ugr.es (M.M. Erenas).

https://doi.org/10.1016/j.talanta.2022.124094
Received 12 September 2022; Received in revised form 3 November 2022; Accepted 6 November 2022
Available online 11 November 2022

lithium determination with blood morphotic elements separation unit made of glass microfiber. Lithium ion was detected using F28 tetraphenylporphyrin reagent [8]. As a step further, a hybrid sensor was introduced, which consisted of digital microfluidic for blood separation and paper-based device for colorimetric lithium determination [9]. Some attempts to miniaturize classical ion selective electrodes were undertaken as well. Novell et al. proposed a microfluidic paper-based potentiometric cell for lithium ion determination in whole blood [10]. Lithium selective membrane and a reference membrane were deposited on paper coated with carbon nanotubes. Besides paper, other solid supports have been used to fabricate potentiometric cells for lithium determination, such as polyimide [11,12] or cotton fiber [13]. Voltammetric techniques have also been used for lithium detection in point-of-care format, utilizing electrodes modified with lithium manganese oxide [14] or functionalized with 6,6′-dibenzyl-14-crown-4 ether (Li ionophore VI) [15]. Finally, several lab-on-a-chip devices employing electrophoresis for lithium determination were reported [16–18].

Optical determination of ionic species can be performed with the aid of chromoionophore-ionophore chemistry. This is a concept known since 1990s and widely used for the determination of various cations and anions [19]. Despite its popularity, ionophore-based optical sensors for lithium detection are rarely reported [20–23] and hardly ever their application to real samples is demonstrated [24,25]. This is probably due to the fact that an exceptional selectivity is required for accurate lithium determination in the presence of 100–300 times higher concentration of sodium in biological matrices. In this paper, ionophore-based chemistry was introduced to a thread-based microfluidic device (μTAD) to create a single-use lithium sensor. Using thread as solid support for ionophore-based sensing has several advantages, such as short response time, flexibility, ease of fabrication and sample pretreatment [26,27].

Here we report a development, optimization and validation of thread-based microfluidic utilizing chromoionophore-ionophore chemistry for salivary lithium determination. To our best knowledge, this is the first described μTAD as well as the first ionophore-based optical sensing device for lithium detection. The required selectivity was ensured by the addition of trioctylphosphine oxide to the sensing cocktail. Such cocktails are widely used in potentiometric lithium ion-selective membranes, but have not been tested in ionophore-based optical sensors so far. The obtained sensors were validated with real saliva samples, demonstrating high accuracy and precision.

2. Experimental

2.1. Reagents and materials

Polyvinyl chloride (PVC), potassium tetrakis [3,5-bis (trifluoromethyl)phenyl]borate (KFMPB), chromoionophore I (liphophilized Nile Blue, ETH 5294), 6,6-dibenzyl-14-crown-4 (Lithium ionophore VI), *o*-nitrophenyloctyl ether (NPOE), dioctyl sebacate (DOS), trioctylphosphine oxide (TOPO), tetrahydrofuran (THF), Tris base and all inorganic salts were obtained from Sigma-Aldrich (Madrid, Spain). Tributyl phosphate (TBP) was purchased from Honeywell Fluka (Madrid, Spain). Purified water (18.2 MΩ cm resistance) was obtained from Milli-RO 12 plus Milli-Q station (Millipore, Bedford, MA, USA) and was used to prepare all aqueous solutions.

White cotton thread (caliber 12 and NTex 94) from Finca (Presencia Hilaturas S.A., Spain), 600 μm of diameter and made up of 250 ± 10 fibres, was used to prepare μTADs after washing it with boiling 10 g L^{-1} sodium carbonate aqueous solution for 1 h, followed by rinsing with distilled water until neutral pH was obtained. Clean thread was then left to dry in room temperature.

2.2. Sensors preparation and analytical signal acquisition

A 2 cm long pieces of thread were cut and glued on double adhesive tape, which was placed on a piece of paper. Then 5 μL of buffer solution (50 mmol L^{-1} TRIS buffer, pH 9.0) was drop casted on each piece of thread and left to dry. After drying, 0.5 μL of sensing cocktail was deposited in the middle of thread sensor. The initial composition of the cocktail was: 0.5 mg (1.0 wt %) chromoionophore I, 0.4 mg (0.8 wt %) Li ionophore VI, 0.7 mg (1.4 wt %) KFMPB, 33.3 mg (64.4 wt %) plasticizer – NPOE, TBP or DOS and 16.7 mg (32.3 wt %) PVC, dissolved in 1 mL of freshly distilled THF. Unless stated otherwise, prior to deposition, the cocktail was diluted 3-fold with THF. To use the thread sensor, 10 μL of sample was introduced at one end of μTAD, triggering a change in protonation state of chromoionophore, resulting in color shift from blue to magenta. Actual photos of the sensors for low (protonated chromoionophore) and high (deprotonated chromoionophore) lithium concentration are shown in Fig. S1 in Electronic Supplementary Information (ESI). All limits of detection was estimated from the intersection of two linear regression– of the flat region and the region of the biggest growth, similarly to IUPAC recommendations for ion-selective electrodes [28].

To precisely measure this color change and limit the influence of outside lightning conditions, the sensors were placed in a custom-made, white illumination box, 23 × 23.5 × 23 cm in size. Consistent lightning was provided by two LED light strips (50 LEDs each – 550 lumens, 5600 K color temperature), located on the opposite edges of the box. The experimental setup is shown in Fig. S1 C. Quantitative measurements were performed by capturing a photo of the sensors with Sony DSC-HX300 camera (Sony, Japan). The parameters of the camera were fixed at the following values: 3648 × 2736 pixel resolution, f/4 aperture value, 1/40 s exposure time, ISO 80, 5600 K white balance. Unless stated otherwise, each measurement was repeated in triplicate, using a new device for each replicate. Error bars presented in all figures represent standard deviations of these three measurements.

The obtained photos were analyzed using ImageJ freeware software (National Institutes of Health, USA). Firstly, photos were transformed from RGB to HSV color space to use H coordinate as the analytical signal [29]. Then a longitudinal section of thread image was selected manually, consisting of ca. 5000 pixels, to acquire average signal from the colored zone and H parameter was measured in this section. For kinetic measurements, videos were recorded instead of photos, and specific frames were extracted using Avidemux software.

2.3. Real and artificial samples analysis

Artificial saliva was prepared according to the recipe given by Gal et al. [30]. Real saliva samples were collected from 10 healthy volunteers using the spitting method [31]. Written informed consent was obtained from all participants before starting the study and the protocol met the requirements of the Declaration of Helsinki and the ethical standards. All samples were spiked with 0.25 mol L^{-1} Li(I) solution to obtain concentration of lithium in the 1–5 mmol L^{-1} range. Spiked samples as well as blank (unspiked) samples were analyzed without any further modifications.

2.4. Reference method

Flame emission photometry was employed as a reference method for lithium analysis [32]. All samples were appropriately diluted with purified water (20–50-fold, depending on their concentration) and measured with flame photometer equipped with lithium filter (Scharlau Science, model PFP7).

3. Results and discussion

3.1. Cocktail composition optimization

The developed μTADs rely on ionophore-chromoionophore chemistry. In this type of sensors, the analyte ion is extracted to the membrane phase to selectively react with ionophore. To maintain electroneutrality

of the membrane, H^+ ion, previously bound to chromoionophore, has to leave the membrane. This process causes a color change of chromoionophore, a lipophilic pH indicator. The recognition process can be summarized in the following equation (1):

$$\overline{L} + \overline{HI^+} + \overline{R^-} + Li^+ \leftrightarrows \overline{I} + \overline{LiL^+} + \overline{R^-} + H^+ \quad (1)$$

For lithium-selective membranes reported here ionophore (L) is 6,6-dibenzyl-14-crown-4, lipophilic pH indicator (I) is lipophilized Nile blue and lipophilic salt (R^-) is potassium tetrakis [3,5-bis(trifluoromethyl) phenyl]borate. Consequently, an exchange constant of this process can be defined, assuming a 1:1 ionophore-analyte complex and +1 charge of analyte ion, where a_H^+ and a_{Li}^+ are activities of hydrogen and lithium ions, respectively, α is the degree of chromoionophore protonation, and C_R, C_I and C_L are molal concentrations of lipophilic salt, indicator and ionophore, respectively:

$$K_{exch} = \frac{a_{H^+}\alpha}{a_{Li^+}(1-\alpha)} \frac{C_R - (1-\alpha)C_I}{C_L - C_R + (1-\alpha)C_I} \quad (2)$$

Usually, the analytical parameter used in this kind of sensors is 1- α, α being the degree of protonation of the chromoionophore. This parameter requires three different measurements (fully protonated signal, fully deprotonated signal, and signal from standard or sample) from the same device to calculate α. To ease the analytical parameter acquisition, when a bitonal optical sensor is used it has been demonstrated that the chromatic coordinate H from the hue-oriented HSV color space can be used as the analytical parameter instead of 1- α [29]. Thank to this color coordinate, only one measurement is required to obtain the analytical parameter. Also, concentration of the analyte will be used instead of activity in this work as no models will be acquired from the data.

Eq (2) indicates that the degree of protonation (α) of I, and consequently, the H parameter depends on exchange constant, concentration of membrane components, concentration of analyte and pH. To maintain every variable but analyte concentration constant and avoid cross-reactivity pH has to be buffered.

Five buffer solutions of pH 4.5 (acetate buffer), 6.0 (phosphate buffer), 7.0, 8.0 and 9.0 (TRIS buffers) were preliminarily screened to establish which one provides the widest measuring range, defined as the difference in H coordinate measured for 10^{-6} and 10^{-1} mol L^{-1} lithium standards. The concentration of each buffer solution was 50 mmol L^{-1}. The cocktail composition is indicated in Section 2.2. With DOS as a plasticizer. The obtained results, shown in Fig. S2 in ESI, clearly point to pH 9.0 TRIS buffer as the one that provides the widest measuring range so it was used in all further experiments.

Very limited data on lithium selective ionophore-based optical sensors is available in the literature thus a detailed optimization of cocktail composition was undertaken. As demonstrated in the literature [24] the type of plasticizer used for membranes preparation has a fundamental influence on the performance of Li-selective optodes. For that reason, three different plasticizers, namely DOS, NPOE and TBP were tested according to the methodology given is ESI (Section S1.1). The obtained results are presented in Fig. 1. Contrary to findings presented in Ref. [24], the response patterns for membranes plasticized with DOS and NPOE are almost the same. Unfortunately, neither DOS nor NPOE are suitable as plasticizers when keeping in mind a potential application of μTAD to lithium determination in saliva samples, because the obtained limits of detection are way above the clinically relevant concentration range, namely 10.2 and 13.6 mmol L^{-1} for DOS and NPOE, respectively. Although providing very good precision, the limit of detection is way too high to allow for lithium determination in biological matrices. On the other hand, despite significantly worse precision, the use of TBP enables the determination of lithium within clinically relevant range therefore it was selected for further experiments. The enhanced sensitivity towards lithium is most likely attributed to the presence of phosphate group in TBP, which facilitates Li(I) extraction to organic phase and therefore improve the detection limit [33].

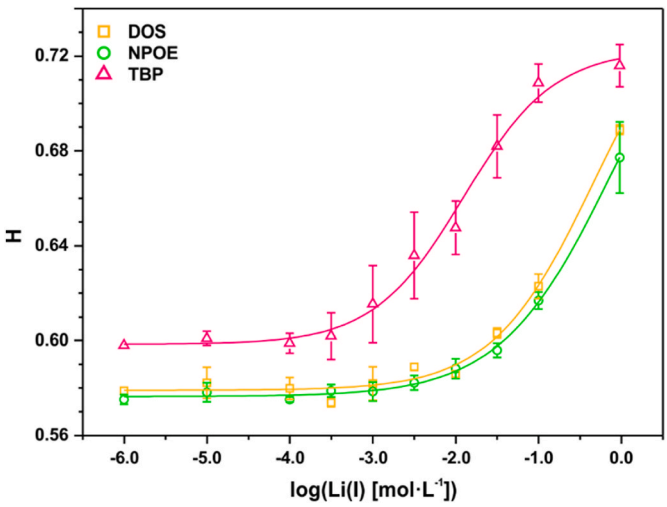

Fig. 1. Calibration dependencies obtained with μTADs plasticized with 3 different plasticizers: DOS – dioctyl sebacate; NPOE – *o*-nitrophenyloctyl ether; TBP – tributyl phosphate, cocktail dilution: 4*x*, n = 3. The fitted curves are Boltzmann sigmoidal functions.

Poor precision for TBP-based cocktail may be attributed to too big dilution factor of the cocktail. On one hand, as shown in earlier studies [26,27], diluting cocktail is necessary to avoid too intense colors of μTADs as it reduces discrimination ability of H coordinate. On the other hand, too diluted cocktail produces very pale color of μTADs, making acquiring a reliable signal difficult. Both of these phenomena significantly affect precision therefore an optimization of dilution factor was undertaken. The details of this study are given in ESI (Section S1.2 and Fig. S3). The results clearly indicate that 3-fold cocktail dilution provides the best precision and the widest measuring range.

Another crucial parameter affecting the response of ionophore-based optical sensors is chromoionophore to lipophilic salt to ionophore (I: R^-: L) molar ratio and so it was subjected to optimization. To begin with, the amount of chromoionophore was set at 16.8 mmol kg^{-1} and kept constant throughout these experiments. First, the amount of lipophilic salt was optimized by registering calibration curves for cocktails with the following I: R^-: L ratios – 1:1:1.5; 1:1.25:1.5 and 1:1.5:1.5 (Section S1.3 and Fig. S4). Out of these compositions, 1:1.25:1.5 provided the biggest sensitivity and the lowest limit of detection. Next, the influence of ionophore content on the μTADs response was studied using cocktails with the following I: R^-: L ratios: 1:1.25:1.0; 1:1.25:1.5; 1:1.25:1.75 and 1:1.25:2.0 (Section S1.4 and Fig. S5). Cocktail with 1:1.25:1.5 I: R^-: L molar ratio was selected as the optimal one due to the widest measuring range.

To conclude, the optimal cocktail consisted of: 0.5 mg (1.0 wt %) chromoionophore I, 0.5 mg (1.0 wt %) Li ionophore VI, 0.92 mg (1.8 wt %) KFMPB, 33.3 mg (64.1 wt %) TBP and 16.7 mg (32.2 wt %) PVC dissolved in 1 mL of THF, resulting in 16.5 mmol kg^{-1} of chromoionophore, 25.0 mmol kg^{-1} of ionophore and 19.6 mmol kg^{-1} of salt. To obtain precise measurements in a wide range of H the cocktail needs to be diluted 3-fold with THF.

3.2. Selectivity and analytical parameters

To obtain a calibration function, ten lithium standards ranging from 10^{-6} to 0.95 mol L^{-1}, were analyzed in five replicates, each with a new μTAD. The shape of the response was, as usual for ionophore-based sensors, sigmoidal (Fig. 2, full points) so a Boltzmann function was fitted to the data set. The details of Boltzmann equation as well as analytical parameters of the μTADs are summarized in Table 1.

The obtained limit of detection (0.33 mmol L^{-1}) indicates that it might be possible to determine lithium in both saliva and blood serum.

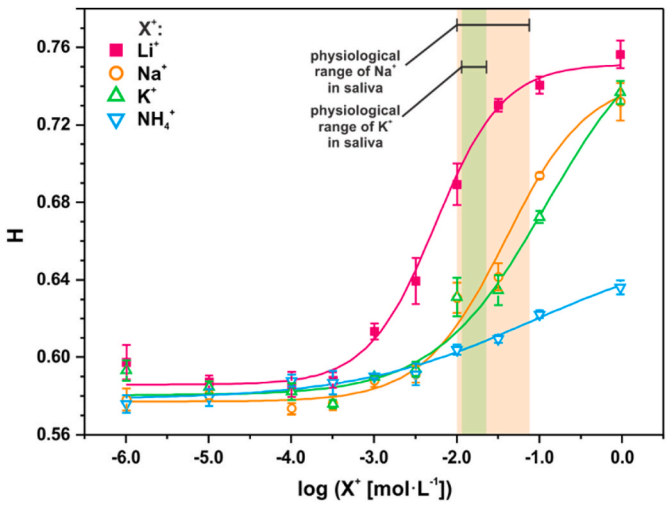

Fig. 2. Selectivity study using separated solution method, n = 3. Physiological ranges of sodium and potassium in saliva were taken from Ref. [34].

Table 1
Boltzmann equation and analytical parameters for lithium μTAD (plasticizer – TBP).

Boltzmann equation $y = \frac{A_1 - A_2}{1 + e^{(x-x_0)/dx}} + A_2$		analytical parameters	
A_1	0.586	Limit of detection	$3.3{\cdot}10^{-4}$ mol L^{-1}
A_2	0.752	Dynamic range	$3.3{\cdot}10^{-4}$ – 0.95 mol L^{-1}
x_0	−2.26	Precision (10^{-3} mol L^{-1})	0.68%
dx	0.409	Precision (10^{-2} mol L^{-1})	1.56%
R^2	0.995	Precision (10^{-1} mol L^{-1})	0.59%

However, another crucial factor which has to be considered is the selectivity of μTADs, especially keeping in mind, that the concentration of potentially interfering ions is a few times bigger than the concentration of lithium. For that reason, the selectivity of μTADs was established using separated solutions method (SSM, see Section S2 for methodological details) [27]. At this stage, the interferents selected to be tested were: sodium, potassium and ammonium cations. The obtained results, shown in Fig. 2, are far from satisfactory. The values of selectivity coefficients (log $K^{opt}_{Li(I)-X(I)}$) were −0.81, −1.28 and −4.36 for sodium, potassium and ammonium ion, respectively. When considering the physiological ranges of sodium and potassium in saliva, marked in Fig. 2, it is clear that an accurate and selective determination of lithium which is at the level of *ca.* 1 mmol L^{-1} in biological matrix is not feasible. Therefore, investigations were undertaken to find a way to boost sensors selectivity.

3.3. Selectivity enhancement

Findings described in Section 3.2. Triggered a search for a way to enhance the selectivity of the developed μTADs. A quite common approach to improve the analytical performance of lithium ion-selective electrodes is an addition of a compound called trioctylphosphine oxide (TOPO) to membrane cocktail, usually around 1.5 wt % [13]. TOPO is a highly effective lithium ion extractant. Research has shown that a significant increase of selectivity of lithium over sodium is achieved when TOPO is added to membrane cocktail. Interestingly, this was not attributed to a decrease in the electrode's response to sodium, but an increase of the response to lithium [35]. However, to our best knowledge, there are no reports about the use of TOPO in ionophore-based optical sensors.

Since the extraction mechanism is similar for ion-selective electrodes and ionophore-based optical sensors, we added 1.5 wt% of TOPO to the optimal cocktail and registered calibration dependencies for lithium and sodium. The selectivity coefficient (log $K^{opt}_{Li(I)-Na(I)}$) changed from −0.81 in the absence of TOPO to −1.15 in the presence of TOPO indicating an improvement of selectivity. However, the selectivity is still insufficient for reliable lithium determination in real samples.

Encouraged by these findings, we further studied the use of TOPO in ion-selective membranes. Since in a vast majority of studies TOPO was used in NPOE-plasticized membranes [13,35], TBP was switched to NPOE as a plasticizer, while leaving all of the other cocktail components in the optimized amounts. Membrane cocktails were prepared with varying content of TOPO – from 0 to 5 wt%. To maintain a constant mass of cocktail components, when weight percentage of TOPO was increased, the weight percentage of NPOE was decreased (i.e. cocktail with 0 wt% TOPO had 64.5 wt % NPOE, cocktail with 1 wt% TOPO had 63.5% NPOE and so on, see Section S3 for details). Calibration curves were registered using μTADs sensitized with the obtained cocktails. The calibration curves, presented in Fig. 3A, reveal that an increasing amount of TOPO enhances the μTADs' response towards lithium. This means that the behavior of TOPO in ionophore-based optical sensors is similar to its behavior in ion-selective electrodes [35]. The addition of TOPO to NPOE-plasticized membranes significantly increased their potential to be used for lithium determination in biological media, compared to a TOPO-free NPOE-plasticized membranes (Fig. 1).

We also conducted a preliminary interference study for sodium (shown in Fig. 3B) and potassium ions (Fig. S6), again using SSM. The obtained results indicate that the presence of TOPO not only enhances μTADs sensitivity towards lithium ion, but also towards interfering ions therefore it is essential to find a compromise between these two processes. Finally, cocktail with 2 wt % TOPO was selected because it provides sufficient sensitivity towards lithium as well as minimal interferences from previously problematic sodium and potassium ions in the physiological range.

3.4. Analytical parameters

After the addition of TOPO, the optimal composition of cocktail is as follows: 1.0 wt % chromoionophore I, 1.0 wt % Li ionophore VI, 1.8 wt % KFMPB, 2.0 wt % TOPO, 62.5 wt % NPOE and 31.8 wt % PVC. Using this cocktail to sensitize μTADs, a calibration curve, shown in Fig. 4, was registered using a new sensor for each replicate. The calibration curve is of sigmoidal shape, but in the tested concentration range a full deprotonation of chromoionophore is not achieved therefore the plateau in the top part of the curve is not apparent. Nonetheless, a Boltzmann function was fitted to the obtained data and its parameters are given in Table 2.

Analytical parameters of the developed μTADs were calculated and are shown in Table 2. Selectivity towards lithium was assessed using separated solutions method and the potential interferents tested were: sodium, potassium, ammonium, calcium and magnesium ions. The response curves are shown in Fig. S7. Sensors did not respond to ammonium ion in the tested range therefore the selectivity coefficient cannot be reported for these ions. The calculated selectivity coefficients indicate exceptional selectivity towards lithium over the tested cations. For all the tested interferents the required selectivity was calculated assuming 10% maximum tolerable error. It is clear that sensors demonstrate sufficient selectivity for accurate lithium determination in saliva. The obtained selectivity coefficient for calcium ion is comparable with the one reported for TOPO-containing lithium ion-selective electrode, while μTAD exhibits superior selectivity for sodium, potassium, ammonium and magnesium ions compared to Li-ISE [36]. This clearly demonstrated that TOPO can successfully be included in ionophore-based optical sensors to boost their selectivity.

The kinetics of reaction between lithium and the membrane was also studied to establish an optimal equilibration time (see Section S5 for

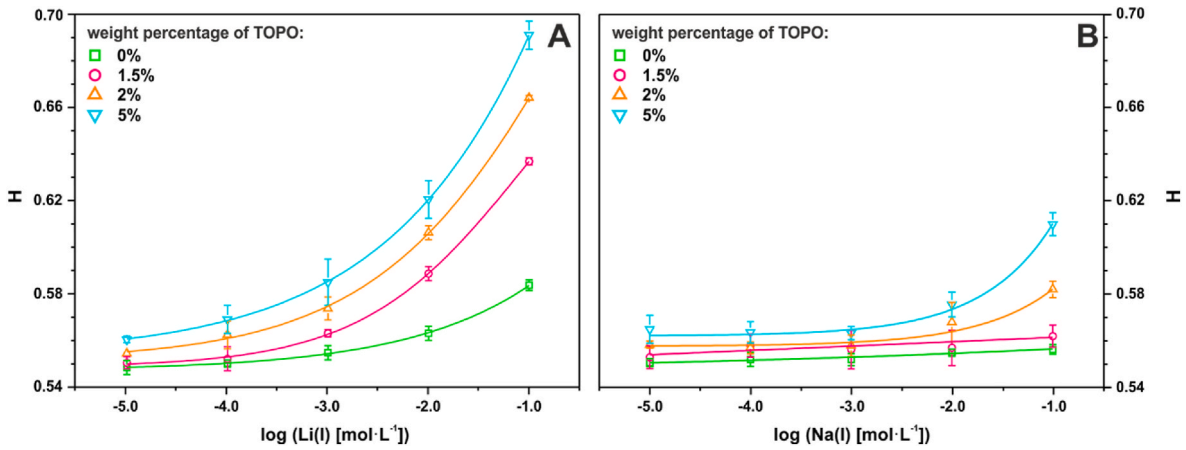

Fig. 3. Optimization of TOPO content in the lithium selective cocktail in terms of selectivity towards lithium (A) and sodium (B), n = 3.

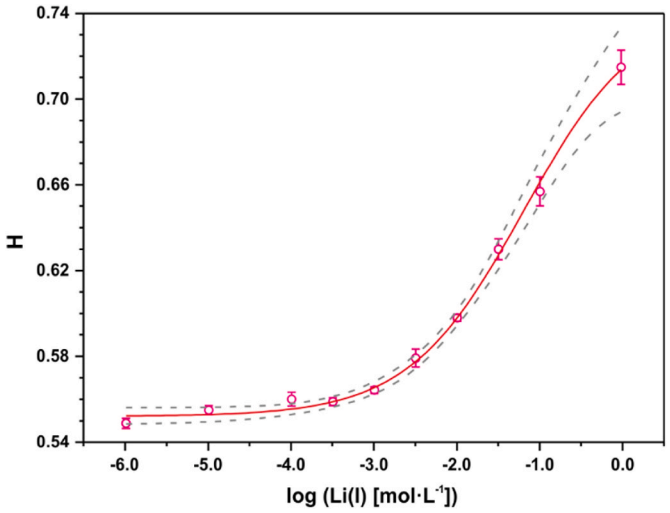

Fig. 4. Calibration curve for μTADs with fitted Boltzmann function, dashed lines represent 95% confidence interval, n = 5.

Table 2
Boltzmann equation, analytical parameters and selectivity coefficients for lithium μTAD (plasticizer – NPOE/TOPO). Required selectivity was calculated for 10% maximum tolerable error according to equation and with assumed minimum and maximum concentrations given in Section S2 in ESI.

Boltzmann equation $y = \frac{A_1 - A_2}{1 + e^{(x-x_0)/dx}} + A_2$		Analytical parameters	
A_1	0.552	Limit of detection	$8.8{\cdot}10^{-4}$ mol L^{-1}
A_2	0.743	Dynamic range	$8.8{\cdot}10^{-4}$ – 0.95 mol L^{-1}
x_0	−1.20	Precision (10^{-3} mol L^{-1})	0.28%
dx	0.695	Precision (10^{-2} mol L^{-1})	0.27%
R^2	0.991	Precision (10^{-1} mol L^{-1})	1.04%
Selectivity		$\log K^{opt}_{Li(I)-NH4(I)}$	–
$\log K^{opt}_{Li(I)-Na(I)}$	−5.96	$\log K^{opt}_{Li(I)-Mg(II)}$	−4.36
$\log K^{opt}_{Li(I)-K(I)}$	−6.74	$\log K^{opt}_{Li(I)-Ca(II)}$	−1.55
Required selectivity		$\log K^{opt}_{Li(I)-NH4(I),req.}$	−0.08
$\log K^{opt}_{Li(I)-Na(I),req.}$	−2.88	$\log K^{opt}_{Li(I)-Mg(II),req.}$	−0.60
$\log K^{opt}_{Li(I)-K(I),req.}$	−2.36	$\log K^{opt}_{Li(I)-Ca(II),req.}$	−1.36

details). The obtained results for two Li standards (Fig. S8 in ESI), namely 1 mmol L^{-1} and 32 mmol L^{-1}, reveal that a steady-state is achieved after *ca.* 10 s after standard introduction and the signal remains stable for at least 5 min.

Additionally, a stability test was conducted to determine a suitable time of μTADs storage without a significant change in their response. Sensors were placed in a black desiccator and the signal for 3.2 mmol L^{-1} lithium standard was measured every few days. Similarly to previous reports [27], μTADs exhibited rather short life-time (defined as the maximal period without statistically significant changes in sensors response) of around 3 days (Fig. S9 in ESI).

A comparison, presented in Table 3, between the developed μTAD with selected lithium sensors reported in the literature reveals that it is comparable in terms of LOD, but offers shorter analysis time and requires lower sample volumes than most sensors.

3.5. Real samples analysis

3.5.1. Validation of the developed sensors for real samples analysis

Additional validation of the developed μTADs was performed using real saliva samples to confirm that lithium can be accurately determined in such complex matrix. First of all, precision of μTADs was established with saliva sample spiked with 3.2 mmol L^{-1} of lithium. The obtained coefficient of variation was 1.17% for 12 replicate measurements. This proves that despite high viscosity and inhomogeneity of saliva, lithium can be determined with satisfactory precision.

Secondly, to confirm that no additional matrix effects are observed when real or artificial samples are tested, calibration curves were registered using lithium standards prepared in water, artificial saliva (prepared according to Ref. [30]) and real saliva (coming from one donor). The obtained results (Fig. 5) clearly suggest a negative interference in both artificial and real saliva for high lithium concentration and some positive interferences for low lithium concentrations, which are irrelevant for salivary lithium determination. The expected errors of lithium concentration determination for real and artificial saliva are −43% and −19%, respectively, for 1 mmol L^{-1} of lithium and −60% and −33%, respectively, for 3.2 mmol L^{-1} of lithium. These do not allow for accurate lithium determination so additional steps to improve selectivity have to be undertaken.

Visual inspection of the reaction progress (i.e. μTAD's color change) hinted that the kinetics of the reaction between lithium and the membrane might be different for lithium in real saliva and for lithium in water. In the former case a color shift from blue to pink is observed initially, but it returns to blue after some time, while in the latter case the color change is stable (see Fig. S8 in ESI). To confirm this finding experimentally, kinetics were registered (see Section S5 for experimental details) for two lithium standards in real saliva – 1 and 10 mmol L^{-1}. The results presented in Fig. 6 and Fig. S8 clearly support the thesis of different reaction kinetics in real sample and in water. Interestingly, the maximum value of hue coordinate registered for real saliva

Table 3
A comparison between the developed μTAD and selected sensors for lithium reported in the literature.

detection method	limit of detection [mmol·L^{-1}]	analysis time [s]	sample	sample volume [μL]	reference
colorimetric	0.054	10	whole blood	20	[8]
colorimetric	0.267	240	whole blood	5	[9]
electrochemical (potentiometric)	1.4	no data	sweat	no data	[12]
electrochemical (potentiometric)	0.011	40	whole blood	50	[10]
electrochemical (linear sweep voltammetry)	0.05	<180	saliva	50	[14]
colorimetric	0.88	10	saliva	10	this work

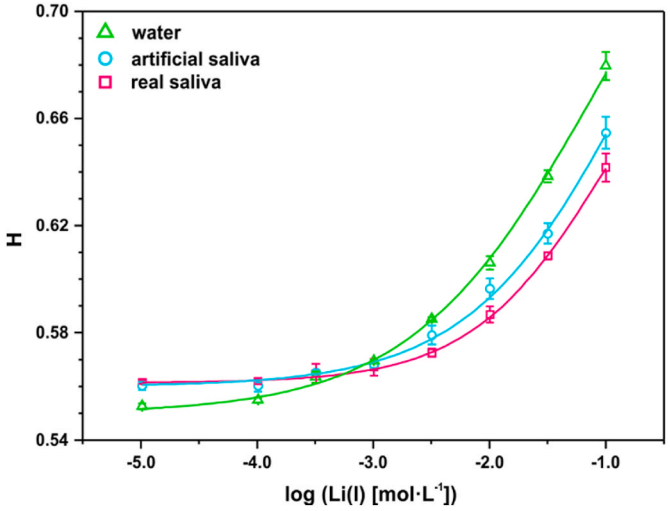

Fig. 5. Calibration dependencies registered using lithium standards prepared in water (triangles), artificial saliva (circles) and real saliva (squares), n = 3.

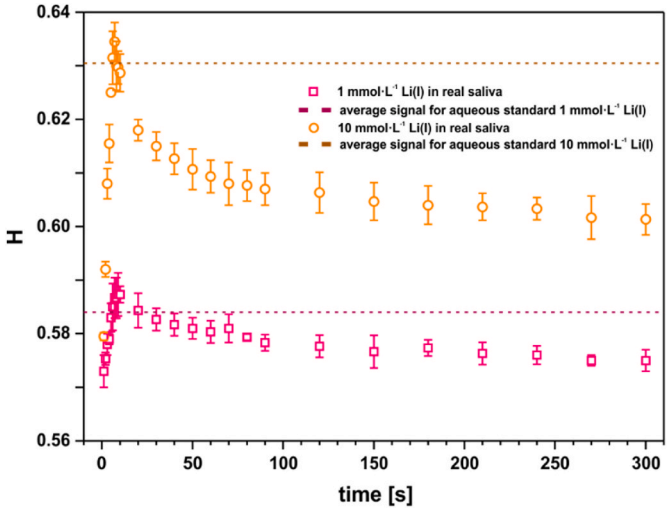

Fig. 6. The influence of equilibration time on the registered signal for low (1 mmol L^{-1}) and high (10 mmol L^{-1}) lithium concentrations in real saliva, n = 3. Dashed lines represent an average signal obtained for aqueous standards with the respective concentration of lithium.

corresponds to hue which is obtained for aqueous standards (marked as dashed lines in Fig. 6). This indicates that in the first stage lithium is extracted to the membrane phase, just like in a matrix-free standard, resulting in chromoionophore deprotonation. Then some competing process occurs, which partially reverses chromoionophore deprotonation and causes a decrease in the measured H. Since such a behavior of ionophore-based optical sensors has not been reported so far, we concluded that it is probably can be associated with the presence of TOPO in the membrane.

TOPO is a quite versatile extracting agent and, when dissolved in an organic solvent, it can be used to extract various organic acids from aqueous to organic phase. According to the literature, TOPO can be employed to extract adipic, succinic, levulinic [37] and acetic acid [38] with very high efficiencies. This is attributed to a hydrogen bond formation between oxygen from phosphate group of TOPO and the OH group from extracted acid. It is therefore possible, that an organic acid is extracted from saliva to the membrane phase with the aid of TOPO. This would result in protonation of chromoionophore, which was previously deprotonated owing to extraction of lithium ion. The mentioned organic acid might be, for example, uric acid [39], acetic acid [40] or lactic acid [41]. All things considered, it seems that the most accurate indicator of lithium concentration in saliva is the maximum measured H in the initial stage of the reaction. This maximum H value can be easily measured by using a smartphone running a custom app that analyses the color change of the μTAD in real time [42]. This demonstrates that the combination of smartphones together with POC devices allows to obtain signal that would be difficult to acquire by untrained personnel.

3.5.2. *Real samples analysis*

Real saliva samples were spiked with lithium chloride to be within therapeutic, below therapeutic or toxic level of lithium. The number of lithium concentrations analyzed for one sample depended on the volume of saliva donated. The samples were analyzed without any further modifications using μTADs. Flame photometry was used as a reference method and the measurements were performed according to the description given in Section 2.4. For μTADs a kinetic mode of measurements was employed – a video of sensors was recorded for each sample. Hue coordinate was measured in frames cut from the video every 1 s for the initial 15 s after sample introduction. Average signal was calculated for 3 sensors and the maximum average H obtained was treated as analytical signal, converted to concentration using calibration curve. To increase accuracy, a calibration curve was constructed from 7 aqueous lithium standards in the range from 0.3 to 10 mmol L^{-1}. The obtained results are shown in Table 4 and Fig. S10. The relative error does not exceed 20% in almost all cases, which is a satisfactory accuracy, allowing for differentiating between too low, therapeutic and too high lithium concentration.

4. Conclusions

In this paper, we reported on a development of a microfluidic thread-based analytical device for lithium determination in saliva. The importance of lithium determination is very high, as ca. 2% of World population is affected by bipolar disorder and a fair share of them is treated with lithium, requiring regular monitoring of its level. The developed sensors exploit chromoionophore-ionophore chemistry, rarely used for lithium quantification. Significant issues with selectivity were resolved by an addition of a lithium extracting agent to membrane cocktail, previously not used in ionophore-based optical sensors. A careful optimization of variables allowed to achieve sensitive and selective lithium detection in disposable format. Using a kinetic mode of measurements, sensors were validated with saliva samples. It should be highlighted that the response time of μTADs is very short, ca. 10 s. Finally, non-

Table 4
Determination of lithium in spiked saliva samples using the developed μTADs and flame photometry as a reference method, n = 3.

sample Nº	Lithium added [mmol·L^{-1}]	Determined concentration – reference [mmol·L^{-1}]	Determined concentration – μTADs [mmol·L^{-1}]	Relative error
1	3.0	3.22	3.09	−4.0%
2	3.0	3.10	2.51	−19.0%
3	1.0	1.13	1.10	−2.7%
	2.0	2.30	2.11	−8.3%
4	3.0	3.26	3.05	−6.4%
	5.0	5.66	5.23	−7.6%
5	2.0	2.35	2.39	1.7%
6	1.0	1.17	1.03	−12.0%
	3.0	3.37	2.88	−14.5%
	2.0	2.25	2.33	3.6%
	5.0	5.61	4.91	−12.5%
8	1.0	1.19	1.17	−1.7%
	2.0	1.94	2.27	17.0%
9	1.0	1.20	1.32	10.0%
	2.0	2.23	2.15	−3.6%
	5.0	5.71	5.73	0.4%
10	1.0	1.09	0.93	−14.7%
	2.0	2.27	1.80	−20.7%

invasiveness of sample collection combined with very low cost of the analytical device and signal readout without specialized equipment contribute to the developed μTADs potential as point-of-care diagnostic tests, adhering to WHO ASSURED guidelines [43]. Additionally, as shown in our previous works [26,42], smartphone with an appropriate application can successfully substitute digital camera in μTADs visualization. This would further increase the potential of developed sensors to be used on-site.

Credit author statement

Izabela Lewinska: Formal Analysis, Conceptualization, Methodology, Writing – original draft, Funding acquisition, Investigation, Visualization **Luis Fermín Capitán-Vallvey**: Conceptualization, Methodology, Writing – original draft, Funding acquisition, Resources, Project administration **Miguel M. Erenas:** Formal Analysis Conceptualization, Methodology, Writing – original draft, Investigation, Visualization, Supervision

Declaration of competing interest

The authors declare that they have no known competing financial interests or personal relationships that could have appeared to influence the work reported in this paper.

Data availability

Data will be made available on request.

Acknowledgements

This work was founded by Spanish “Ministerio de Economía y Competitividad” (Projects PID2019-103938RB-I00) and Junta de Andalucía (Projects B-FQM-243-UGR18 and P18-RT-2961). The projects were partially supported by European Regional Development Funds (ERDF). These investigations were also supported by Polish National Science Centre (Project PRELUDIUM no. 2021/41/N/ST4/00299).

Appendix A. Supplementary data

Supplementary data to this article can be found online at https://doi.org/10.1016/j.talanta.2022.124094.

References

[1] X. Pérez de Mendiola, D. Hidalgo-Mazzei, E. Vieta, A. González-Pinto, Overview of lithium's use: a nationwide survey, Int. J. Bipolar Disord. 9 (2021), https://doi.org/10.1186/s40345-020-00215-z.
[2] A. Fagiolini, R. Forgione, M. Maccari, A. Cuomo, B. Morana, M.C. Dell'Osso, F. Pellegrini, A. Rossi, Prevalence, chronicity, burden and borders of bipolar disorder, J. Affect. Disord. 148 (2013) 161–169, https://doi.org/10.1016/j.jad.2013.02.001.
[3] M. Gitlin, Lithium side effects and toxicity: prevalence and management strategies, Int. J. Bipolar Disord. 4 (2016), https://doi.org/10.1186/s40345-016-0068-y.
[4] G.M. Goodwin, Evidence-based guidelines for treating bipolar disorder: recommendations from the British Association for Psychopharmacology, J. Psychopharmacol. 17 (2003) 149–173, https://doi.org/10.1177/0269881103017002003.
[5] M. Sheikh, M. Qassem, I.F. Triantis, P.A. Kyriacou, Advances in therapeutic monitoring of lithium in the management of bipolar disorder, Sensors 22 (2022), https://doi.org/10.3390/s22030736.
[6] S.J. Shetty, P.B. Desai, N.M. Patil, R.B. Nayak, Relationship between serum lithium, salivary lithium, and urinary lithium in patients on lithium therapy, Biol. Trace Elem. Res. 147 (2012) 59–62, https://doi.org/10.1007/s12011-011-9295-3.
[7] G.M. Parkin, M.J. McCarthy, S.H. Thein, H.L. Piccerillo, N. Warikoo, D.A. Granger, E.A. Thomas, Saliva testing as a means to monitor therapeutic lithium levels in patients with psychiatric disorders: identification of clinical and environmental covariates, and their incorporation into a prediction model, Bipolar Disord. 23 (2021) 679–688, https://doi.org/10.1111/bdi.13128.
[8] T. Komatsu, M. Maeki, A. Ishida, H. Tani, M. Tokeshi, Paper-based device for the facile colorimetric determination of lithium ions in human whole blood, ACS Sens. 5 (2020) 1287–1294, https://doi.org/10.1021/acssensors.9b02218.
[9] T. Komatsu, M. Tokeshi, S.K. Fan, Determination of blood lithium-ion concentration using digital microfluidic whole-blood separation and preloaded paper sensors, Biosens. Bioelectron. 195 (2022), 113631, https://doi.org/10.1016/j.bios.2021.113631.
[10] M. Novell, T. Guinovart, P. Blondeau, F.X. Rius, F.J. Andrade, A paper-based potentiometric cell for decentralized monitoring of Li levels in whole blood, Lab Chip 14 (2014) 1308–1314, https://doi.org/10.1039/c3lc51098k.
[11] F. Criscuolo, F. Cantu, I. Taurino, S. Carrara, G. De Micheli, Flexible sweat sensors for non-invasive optimization of lithium dose in psychiatric disorders, Proc. IEEE Sensors (2019) 1–4, https://doi.org/10.1109/SENSORS43011.2019.8956598.
[12] F. Criscuolo, I. Ny Hanitra, S. Aiassa, I. Taurino, N. Oliva, S. Carrara, G. De Micheli, Wearable multifunctional sweat-sensing system for efficient healthcare monitoring, Sensor. Actuator. B Chem. 328 (2021), 129017, https://doi.org/10.1016/j.snb.2020.129017.
[13] M.N. Sweilam, J.R. Varcoe, C. Crean, Fabrication and optimization of fiber-based lithium sensor: a step toward wearable sensors for lithium drug monitoring in interstitial fluid, ACS Sens. 3 (2018) 1802–1810, https://doi.org/10.1021/acssensors.8b00528.
[14] A.L. Suherman, B. Rasche, B. Godlewska, P. Nicholas, S. Herlihy, N. Caiger, P. J. Cowen, R.G. Compton, Electrochemical detection and quantification of lithium ions in authentic human saliva using LiMn2O4-modified electrodes, ACS Sens. 4 (2019) 2497–2506, https://doi.org/10.1021/acssensors.9b01176.
[15] U. Singh, S. Kumbhat, Ready to use electrochemical sensor strip for point-of-care monitoring of serum lithium, Electroanalysis 33 (2021) 393–399, https://doi.org/10.1002/elan.202060393.
[16] E.X. Vrouwe, R. Luttge, I. Vermes, A. Van Den Berg, Microchip capillary electrophoresis for point-of-care analysis of lithium, Clin. Chem. 53 (2007) 117–123, https://doi.org/10.1373/clinchem.2007.073726.
[17] P. Kubáň, P.C. Hauser, Evaluation of microchip capillary electrophoresis with external contactless conductivity detection for the determination of major inorganic ions and lithium in serum and urine samples, Lab Chip 8 (2008) 1829–1836, https://doi.org/10.1039/b802973c.
[18] A. Floris, S. Staal, S. Lenk, E. Staijen, D. Kohlheyer, J. Eijkel, A. Van Den Berg, A prefilled, ready-to-use electrophoresis based lab-on-a-chip device for monitoring lithium in blood, Lab Chip 10 (2010) 1799–1806, https://doi.org/10.1039/c003899g.
[19] G. Mistlberger, G.A. Crespo, E. Bakker, Ionophore-based optical sensors, Annu. Rev. Anal. Chem. 7 (2014) 483–512, https://doi.org/10.1146/annurev-anchem-071213-020307.
[20] M. Bocheńska, Design and characterization of a Li-selective optical sensor, J. Inclusion Phenom. Mol. Recognit. Chem. 22 (1995) 269–275, https://doi.org/10.1007/BF00707779.
[21] X. Du, L. Yang, W. Hu, R. Wang, J. Zhai, X. Xie, A plasticizer-free miniaturized optical ion sensing platform with ionophores and silicon-based particles, Anal. Chem. 90 (2018) 5818–5824, https://doi.org/10.1021/acs.analchem.8b00360.
[22] K. Suzuki, E. Hirayama, T. Sugiyama, K. Yasuda, H. Okabe, D. Citterio, Ionophore-based lithium ion film optode realizing multiple color variations utilizing digital color analysis, Anal. Chem. 74 (2002) 5766–5773, https://doi.org/10.1021/ac0259414.
[23] E. Hirayama, T. Sugiyama, H. Hisamoto, K. Suzuki, Visual and colorimetric lithium ion sensing based on digital color analysis, Anal. Chem. 72 (2000) 465–474, https://doi.org/10.1021/ac990588w.
[24] M.I. Albero, J.A. Ortuño, M.S. García, M. Cuartero, M.C. Alcaraz, Novel flow-through bulk optode for spectrophotometric determination of lithium in pharmaceuticals and saliva, Sensor. Actuator. B Chem. 145 (2010) 133–138, https://doi.org/10.1016/j.snb.2009.11.053.

[25] K. Watanabe, E. Nakagawa, H. Yamada, H. Hisamoto, K. Suzuki, Lithium ion selective optical sensor based on a novel neutral ionophore and a lipophilic anionic dye, Anal. Chem. 65 (1993) 2704–2710, https://doi.org/10.1021/ac00067a028.
[26] M.J. Arroyo, M.M. Erenas, I. de Orbe-Payá, K. Cantrell, J.A. Dobado, P. Ballester, P. Blondeau, A. Salinas-Castillo, L.F. Capitán-Vallvey, Thread based microfluidic platform for urinary creatinine analysis, Sensor. Actuator. B Chem. 305 (2020), 127407, https://doi.org/10.1016/j.snb.2019.127407.
[27] M.M. Erenas, I. De Orbe-Payá, L.F. Capitan-Vallvey, Surface modified thread-based microfluidic analytical device for selective potassium analysis, Anal. Chem. 88 (2016) 5331–5337, https://doi.org/10.1021/acs.analchem.6b00633.
[28] R.P. Buck, E. Lindner, Recomendations for nomenclature of ion-selective electrodes (IUPAC recommendations 1994), Pure Appl. Chem. 66 (1994) 2527–2536, https://doi.org/10.1351/pac199466122527.
[29] K. Cantrell, M.M. Erenas, I. De Orbe-Payá, L.F. Capitán-Vallvey, Use of the hue parameter of the hue, saturation, value color space as a quantitative analytical parameter for bitonal optical sensors, Anal. Chem. 82 (2010) 531–542, https://doi.org/10.1021/ac901753c.
[30] J.Y. Gal, Y. Fovet, M. Adib-Yadzi, About a synthetic saliva for in vitro studies, Talanta 53 (2001) 1103–1115, https://doi.org/10.1016/S0039-9140(00)00618-4.
[31] F.G. Bellagambi, T. Lomonaco, P. Salvo, F. Vivaldi, M. Hangouët, S. Ghimenti, D. Biagini, F. Di Francesco, R. Fuoco, A. Errachid, Saliva sampling: methods and devices. An overview, TrAC, Trends Anal. Chem. 124 (2020), 115781, https://doi.org/10.1016/j.trac.2019.115781.
[32] A.L. Levy, E.M. Katz, Comparison of serum lithium determinations by flame photometry and atomic absorption spectrophotometry, Clin. Chem. 16 (1970) 840–842, https://doi.org/10.1093/clinchem/16.10.840.
[33] Z. Zhou, W. Qin, W. Fei, Extraction equilibria of lithium with tributyl phosphate in three diluents, J. Chem. Eng. Data 56 (2011) 3518–3522, https://doi.org/10.1021/je200803h.
[34] J. Pytko-Polonczyk, A. Jakubik, A. Przeklasa-Bierowiec, B. Muszynska, Artificial saliva and its use in biological experiments, J. Physiol. Pharmacol. 68 (2017) 807–813.
[35] R.Y. Xie, G.D. Christian, Lithium ion-selective electrodes containing TOPO: determination of serum lithium by flow injection analysis, Analyst 112 (1987) 61–64, https://doi.org/10.1039/AN9871200061.
[36] F. Coldur, M. Andac, A flow-injection potentiometric system for selective and sensitive determination of serum lithium level, Electroanalysis 25 (2013) 732–740, https://doi.org/10.1002/elan.201200466.
[37] E. Riveiro, B. González, Á. Domínguez, Extraction of adipic, levulinic and succinic acids from water using TOPO-based deep eutectic solvents, Separ. Purif. Technol. 241 (2020), 116692, https://doi.org/10.1016/j.seppur.2020.116692.
[38] J. Grilc, V. Golob, B. Zadnlk, Extraction of acetic acid from dilute aqueous solutions with trioctylphosphine oxide, Ind. Eng. Chem. Process Des. Dev. 20 (1981) 433–435, https://doi.org/10.1021/i200014a004.
[39] J.L. Riis, C.I. Bryce, M.J. Matin, J.L. Stebbins, O. Kornienko, L. Van Huisstede, D. A. Granger, The validity, stability, and utility of measuring uric acid in saliva, Biomarkers Med. 12 (2018) 583–596, https://doi.org/10.2217/bmm-2017-0336.
[40] R.M. Effros, R. Casaburi, J. Su, M. Dunning, J. Torday, J. Biller, R. Shaker, The effects of volatile salivary acids and bases on exhaled breath condensate pH, Am. J. Respir. Crit. Care Med. 173 (2006) 386–392, https://doi.org/10.1164/rccm.200507-1059OC.
[41] G. Palleschi, M.H. Faridnia, G.J. Lubrano, G.G. Guilbault, Determination of lactate in human saliva with an electrochemical enzyme probe, Anal. Chim. Acta 245 (1991) 151–157, https://doi.org/10.1016/S0003-2670(00)80215-9.
[42] M.M. Erenas, B. Carrillo-Aguilera, K. Cantrell, S. Gonzalez-Chocano, I.M. Perez de Vargas-Sansalvador, I. de Orbe-Payá, L.F. Capitan-Vallvey, Real time monitoring of glucose in whole blood by smartphone, Biosens, Bioelectron 136 (2019) 47–52, https://doi.org/10.1016/j.bios.2019.04.024.
[43] K.J. Land, D.I. Boeras, X.S. Chen, A.R. Ramsay, R.W. Peeling, REASSURED diagnostics to inform disease control strategies, strengthen health systems and improve patient outcomes, Nat. Microbiol. 4 (2019) 46–54, https://doi.org/10.1038/s41564-018-0295-3.